(Preprint) AAS 15-223

HIGH ALTITUDE VENUS OPERATIONS CONCEPT TRAJECTORY DESIGN, MODELING, AND SIMULATION

Rafael A. Lugo,[*] Thomas A. Ozoroski,[†] John W. Van Norman,[†] Dale C. Arney,[‡] John A. Dec,[§] Christopher A. Jones,[‡] and Carlie H. Zumwalt[**]

A trajectory design and analysis that describes aerocapture, entry, descent, and inflation of manned and unmanned High Altitude Venus Operation Concept (HAVOC) lighter-than-air missions is presented. Mission motivation, concept of operations, and notional entry vehicle designs are presented. The initial trajectory design space is analyzed and discussed before investigating specific trajectories that are deemed representative of a feasible Venus mission. Under the project assumptions, while the high-mass crewed mission will require further research into aerodynamic decelerator technology, it was determined that the unmanned robotic mission is feasible using current technology.

INTRODUCTION

For decades, Mars has been the prime destination for a variety of robotic science missions as well as a target for human exploration. However, there are a number of challenges in executing a manned Mars mission: transit times are significant (as much as a year each way), the surface environment is harsh with low ambient temperatures and pressures, and the surface radiation environment is hazardous to crew health. Venus, conversely, has a shorter transit time (approximately 100 days outbound and up to 300 days inbound) with comparable requirements on in-space propulsion systems. While the surface of Venus presents an environment with temperatures and pressures too great to permit surface platforms to survive for any length of time with current technologies, the atmosphere at approximately 50 km altitude is one of the more hospitable environments in the solar system; the ambient temperature and pressure are much closer to that on the surface of Earth. Radiation protection for the crew is provided by the atmosphere, and a life-supporting mixture of gas similar to air could dually serve as a lifting gas. The Venus Exploration Analysis Group[1] (VEXAG) and the Planetary Science Decadal Survey[2] have also identified planetary science questions that may only be answered from operations in the Venusian atmosphere.

The present work is in support of a NASA Langley Research Center (LaRC) study to consider a conceptual design of an atmospheric platform that would be capable of supporting both human

[*] Flight Mechanics Engineer, Analytical Mechanics Associates, Inc., Hampton, VA, 23666.
[†] Aerospace Engineer, Analytical Mechanics Associates, Inc., Hampton, VA, 23666.
[‡] Aerospace Engineer, Space Mission Analysis Branch, NASA Langley Research Center, Hampton, VA 23681.
[§] Aerospace Engineer, Structural & Thermal Systems Branch, NASA Langley Research Center, Hampton, VA 23681.
[**] Aerospace Engineer, Atmospheric Flight & Entry Systems Branch, NASA Langley Research Center, Hampton, VA 23681.

and robotic missions. This study of a High Altitude Venus Operational Concept (HAVOC) considers the goals, requirements, and systems to explore Venus using both robotic precursor and manned vehicles. A lighter-than-air (LTA) vehicle, or airship, offers the capability of meeting the study's objectives. Analysis of the aerocapture and entry, descent, and inflation trajectories is critical to developing the concept for the airship and its associated atmospheric entry systems.

The present paper will focus on the design, modeling, simulation, and analysis of the two primary segments of the HAVOC trajectories: aerocapture, and entry, descent, and inflation (EDI). During aerocapture the vehicle takes advantage of the drag created by flying through the atmosphere to reduce the speed of the vehicle, without the use of a large propulsive maneuver. Bank angle modulation is used to adjust the lift vector and guide the vehicle toward the desired target apoapsis, using a small propulsive burn to clean up any targeting errors. Once the vehicle is in the desired circular orbit, atmospheric entry may begin. During entry, the entry vehicle (EV) is guided through the middle and lower atmosphere and may be maneuvered to prevent excessive heating and aerodynamic loads. Once the EV has slowed to supersonic velocities, the descent phase begins when an aerodynamic decelerator, such as a parachute or ballute, is deployed to further reduce descent rate. The inflation phase begins when the EV velocity is sufficiently reduced such that the airship may be exposed to the oncoming flow. The airship is pressurized during parachute descent and reaches a nominal altitude of approximately 50 km. Figure 1 shows the HAVOC concept of operations from aerocapture to inflation and operations. Though not shown in the figure, the manned mission requires two vehicles to undergo aerocapture: the crew and airship/cargo are launched separately and arrive at Venus in separate vehicles, then rendezvous in orbit before performing the EDI maneuver.

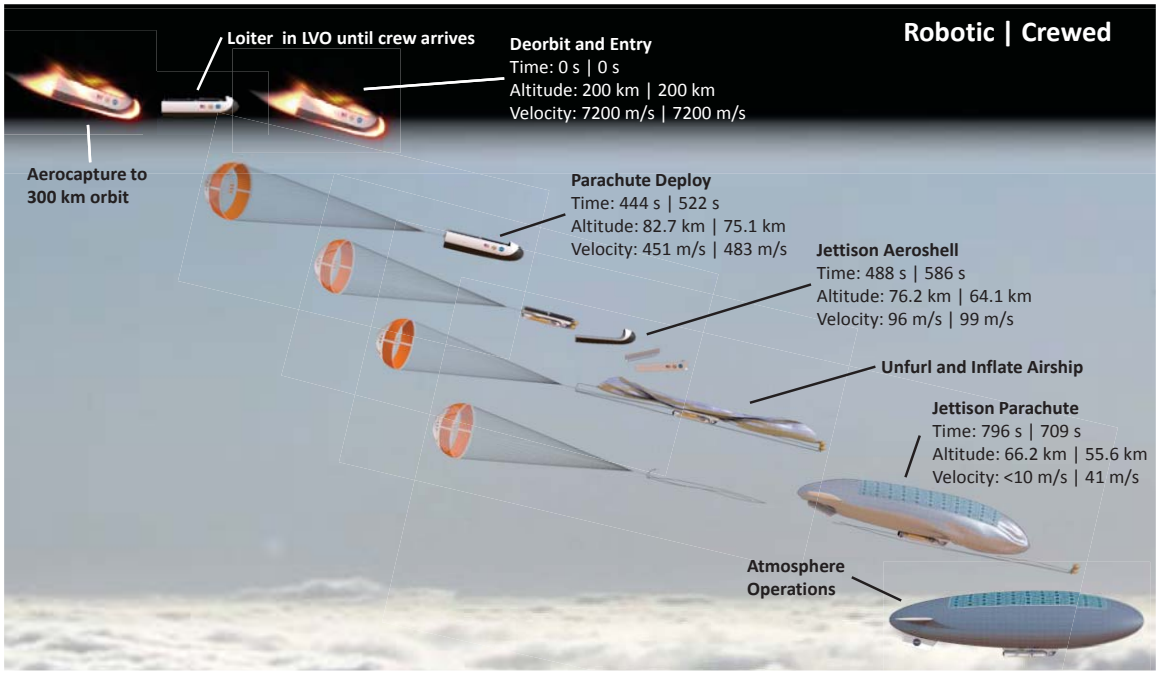

Figure 1. HAVOC Concept of Operations.

TRAJECTORY DESIGN, MODELING, AND SIMULATION

Design and analyses of the entry and descent phases of the trajectories were conducted using the Program to Optimize Simulated Trajectories II (POST2).[3,4] Three-degree-of-freedom simula-

tions run with POST2 used aerodynamic and aeroheating databases generated with CBAERO for the scaled mid-L/D "ellipsled" from the NASA Entry, Descent, and Landing Systems Analysis (EDLSA) study.[5]

The nominal atmosphere was modeled using VenusGRAM 2005[6] assuming no winds. The Venus gravitational field was modeled up to the J4 zonal harmonic. Entry interface was defined as a geodetic altitude of 200 km, and the entry point was defined as the intersection of the equator and the Venus prime meridian (0° latitude, 0° longitude).

Figure 2 shows nominal atmospheric density, pressure, and temperature profiles of Venus obtained from VenusGRAM 2005. The conditions at 50 km altitude are roughly equivalent (though warmer) to atmospheric conditions at sea level on Earth; the nominal density, pressure, and temperature are 1.5948 kg/m^3, 106,679 Pa (1.0528 atm), and 350 K (170°F), respectively. Airship operations are therefore designed for 50 km.

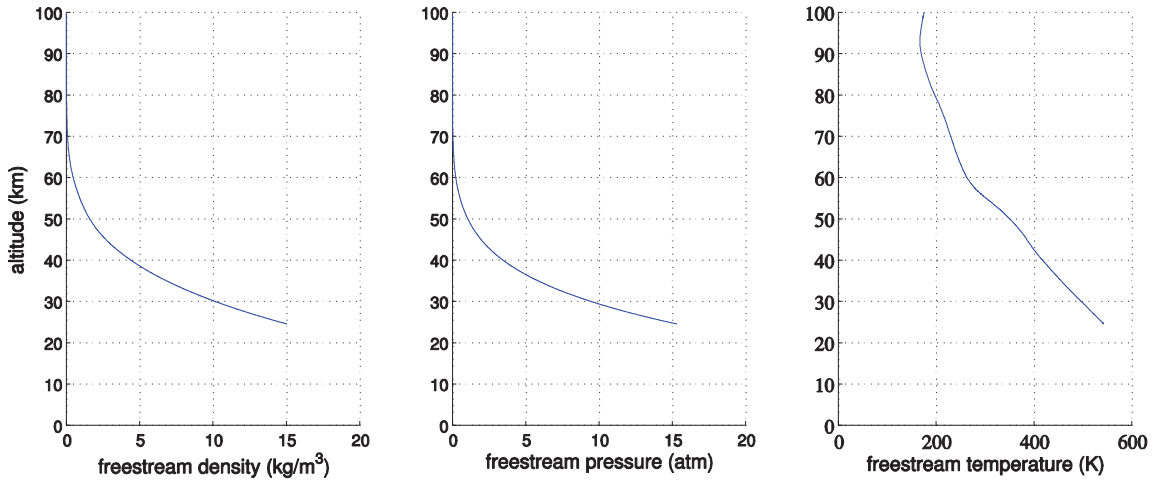

Figure 2. Nominal atmospheric profile of Venus, mid to high altitudes.

The sharp density gradient, coupled with the very high entry mass of the manned mission, present significant trajectory design challenges. Among these are:

1. *Atmosphere skip-out*. Skip-out results when the EV is traveling at too high a velocity (or has too much lift) to be "captured" and exits the atmosphere at a reduced speed, and may or may not re-enter. When controlled, this may be used as a technique for aerocapture and aerobraking.
2. *Excessive lofting*. Lofting is a repeated increase and decrease in altitude due to excessive lift that may result in atmosphere skip-out, and is usually more pronounced in trajectories with shallow entry flight path angles.
3. *Excessive aerodynamic forces (g-loads)*. Excessive g-loads may injure crewmembers and can be fatal at high levels over extended periods. For this reason, NASA has established g-load limits for human crews that are functions of length of exposure and orientation of the crew relative to the acceleration vector.[7]
4. *Excessive aerodynamic heating*. Atmospheric entries are characterized by high heat rates and loads that require the use of thermal protection systems (TPS) to dissipate heat and protect the EV. It is advantageous to minimize heat rates and loads, thereby reducing structural mass.

To address these challenges, a variety of different trajectories were analyzed by establishing a parameter design space and varying specific independent parameters relating to the trajectory. The result was thousands of simulated trajectories from which parameters of interest were extracted and analyzed for trends. The independent parameters of interest were entry flight path angle, total angle of attack, and bank angle. Dependent parameters of interest included peak g-load, peak heat rate, and total heat load. A trajectory was considered "valid" if it did not skip out and if the peak g-load did not exceed predetermined limits. Peak heat rates were monitored, though not used as a selection criteria, since the thermal protection system is designed around these values.

Initial analyses were conducted with an unguided vehicle with a theoretical control system that maintained a constant total angle of attack and bank angle through the trajectory. A target "landing" location was not considered due to the highly mobile nature of the payload/airship, which does not require injection at a precise altitude or latitude. Later analyses implemented a simple logic algorithm to modulate bank angle to mitigate aerodynamic loads.

Aeroshell and Airship Modeling

Initial trajectory designs assumed discrete aeroshells for both aerocapture and EDI, that is, the aerocapture aeroshell would be jettisoned prior to EDI. As the design of the payload matured and the overall mass of the system increased, it was determined that the initial design would not be capable of supporting the heating values predicted by the simulation for either aerocapture or EDI. Other decelerator concepts were explored and a rigid mid-L/D vehicle was selected that would be able to accommodate the mass of the system as well as the two heat pulses that result from two distinct passes through the Venus atmosphere. As will be discussed in the present work, the current designs feature a single aeroshell for both aerocapture and entry with a thermal protection system tailored to the modeled surface heat distribution.

Figure 3 shows notional aeroshell and airship designs. Relevant design parameters for the entry vehicle aeroshells are listed in Table 1.

Figure 3. Notional entry vehicle aeroshell (left) and airship (right) designs. Images are not to relative scale.

Table 1. Entry vehicle parameters.

Parameter	Unit	Unmanned	Manned
Diameter	m	4.7	10.0
Entry mass	mt	4.537	133.9

Both HAVOC airship concepts (unmanned and manned) were sized using the SolFlyte-LTA sizing utility. SolFlyte was developed within the Aeronautics Systems Analysis Branch (ASAB) at NASA Langley Research Center for modeling vehicles and extended-duration missions carried out utilizing solar-electric LTA concepts. The model provides robust, general, rapid sizing estimates and iterative parametric design capability. Key input and output specifications from the LTA sizing utility were used as the basis to formulate the HAVOC inflation and descent modeling capability.

The existing Earth-based airship sizing and operational methodology was slightly modified to reflect the specific requirements of the Venus-based HAVOC concept. Determining airship weight and volume required implementing conversion factors related to differences in gravity, atmospheric molecular weight, and buoyancy. The specific buoyancy of the lifting gas was used to transform the Earth-based design atmosphere density of 1.15 kg/m^3 to a Venus-based density of 1.0914 kg/m^3 that corresponds to altitudes near 50 km. Calculated design volumes of the HAVOC airship concepts were 1,118 m^3 and 77,521 m^3 for the robotic and human missions, respectively. Calculated total masses of the airships, including lifting gas and tanks were 1,382 kg and 95,776 kg for robotic and human missions, respectively.

A significant design consideration became apparent during initial assessments of the human mission. Airship designs do not typically include a requirement to transport lifting gas from one planet to another. In fact, ground-based inflation factors into airship design as an operational constraint. For the HAVOC mission, however, transporting the lifting gas mass to Venus presents a significant payload constraint. The HAVOC crewed mission requires transporting 8,200 kg of helium lifting gas, not including tanks. If it were desirable to use a mixture of gases similar to air as both the lifting gas and a means of life support, 59,400 kg of the gas mixture would be required. Thus, for a human mission, reducing the spacecraft payload mass dictates utilizing the lowest molecular weight lifting gas capable of life support. Though not considered in the present analysis, it will be of interest to investigate the use of a dual-purpose helium-oxygen mixture for the manned mission.

Aerodynamics and Aerothermodynamics

The vehicle outer mold line (OML) considered for the aerocapture and entry phases of flight is an axisymmetric ellipsled based on that of the ELDSA[5] and Design Reference Architecture 5.0 (DRA-5)[8] studies. The configuration may be described as a right circular cylinder with a hemispherical nose cap and flat base, where the baseline exploration-class or manned vehicle has a diameter of 10 meters and overall length of 30 meters, and the robotic-class vehicle dimensions are downscaled to 47% of the baseline. Note that the aeroshell design in Figure 3 is notional and shown for illustrative purposes, and is more complex than the aerodynamic model used in the analysis described here.

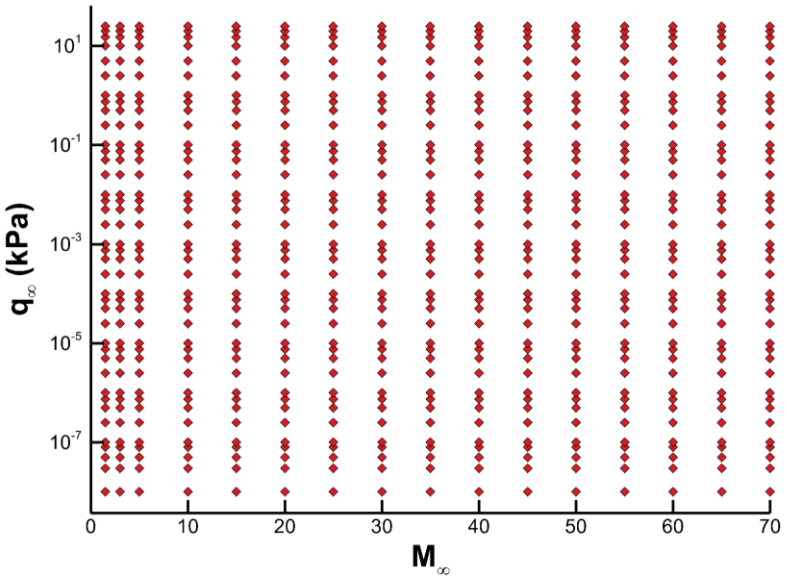

Figure 4. Mach number and dynamic pressure combinations used for CBAERO solutions.

Aerodynamic and aerothermodynamic databases for both exploration- and robotic-class ellipsleds were generated using the Configuration Based Aerodynamics (CBAERO) code.[9] Solutions were computed over a matrix of Mach number and dynamic pressure combinations ranging from free-molecular aerocapture to low supersonic continuum regime conditions as shown in Figure 4, where the transition between free molecular and continuum computations was blended automatically based upon an internal calculation of Knudsen number. At each point, solutions were computed for total angles of attack ranging from 0° to 60° in increments of 10°. A Venus atmosphere model extending to 250 km altitude was used for atmospheric properties including temperature, pressure, ratio of specific heats, and molecular weight. Radiative heating environments were predicted with a Tauber-Sutton correlation,[10] while fully turbulent flow and a fully catalytic wall boundary condition were assumed for conservative convective heating estimates. No control surfaces were modeled, as the corresponding sizing and requisite control algorithms were considered beyond the scope of this study. Point checks for aeroheating and aerodynamics were computed at representative Mach 24 entry conditions using the LAURA[11] and OVERFLOW[12] CFD codes, respectively, and were in good agreement with CBAERO results.

Aerocapture

For the purposes of this study, the aerocapture maneuver is designed to take each vehicle from arrival speeds of approximately 10 to 12 km/s to the roughly 7 km/s velocity necessary to hit the desired orbit apogee. During the pass through the atmosphere, bank angle modulation is used to adjust the lift vector and ensure the vehicle hits the target orbit with minimal error. A simplified bank angle profile is implemented to emulate the flight performance of the vehicle while allowing for the rapid generation of trajectories.

In order to understand the conditions experienced by each vehicle, a design space was developed exploring combinations of input parameters including arrival velocity, target orbit, system mass, and lift-to-drag ratio (L/D). One design space was created for each of the three systems included in this study: one for the robotic mission and two for the manned mission (recall that the crew and airship/cargo arrive at Venus in separate vehicles). To fully characterize the design space, trajectories were generated which would produce minimum and maximum values of all the desired output parameters for each combination of inputs. This was completed by examining the aerocapture corridor. For each combination of inputs, the corridor is bound by flying one trajectory with the lift vector pointing up the entire pass (bank angle of 0°) and then iterating on the entry flight path angle value which allows that trajectory to hit the apoapsis target, then repeating the process for a pass with the lift vector pointing down (bank angle of 180°). These are referred to as the steep and shallow trajectories, respectively, and bound the possible range of flight conditions experienced by the vehicle during aerocapture. One corridor was generated for each combination of inputs described above and this process was repeated for each of the three systems considered for this study.

Trajectory outputs from the three sets of corridors were used to determine which set of inputs, for each vehicle, would produce the desired nominal conditions. Contour plots, demonstrated in Figure 5, were generated for each system to examine conditions such as peak g-loads, peak heat rates, and dynamic pressures. Using the mission constraints imposed on these conditions, one nominal trajectory was generated for each of the three systems to be used for TPS sizing. A simplified bank angle profile was implemented for the nominal trajectory, which involves flying the vehicle with the lift vector pointing directly up (bank angle of 0°) in order to bleed energy from the trajectory without incurring excessive g-loads and heating rates, and then reorienting the vehicle with lift vector pointing down (bank angle of 180°) once peak dynamic pressure has passed, in

order to continue to bleed energy until the desired exit velocity is reached. This method produces three nominal trajectories, one for each system, from which iterations on the design could begin.

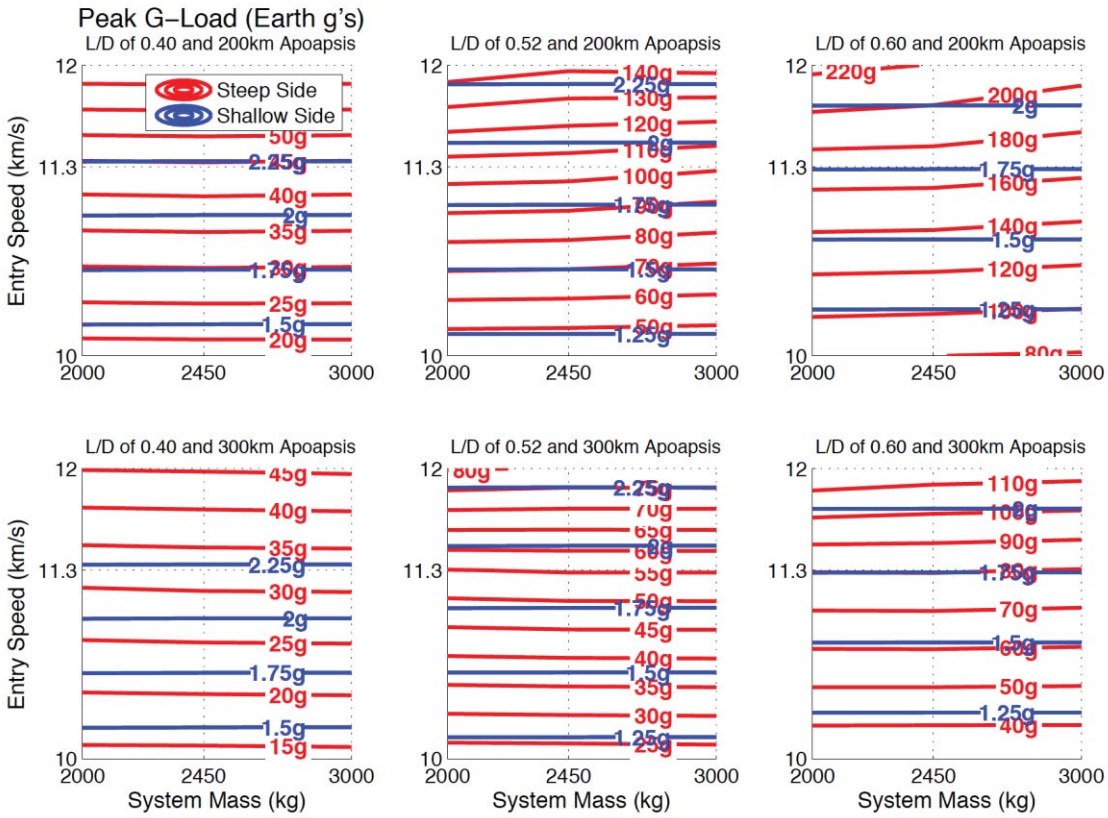

Figure 5. Sample contour of output parameters for HAVOC robotic mission.

Entry and Descent

The entry and descent (ED) portion of the trajectory begins at entry interface (200 km) and, for the purposes of the present analysis, terminates at supersonic parachute deploy (Mach 2.1). The following assumptions were made to facilitate fast analysis of the ED trajectory design space:

1. A constant total angle of attack, selected to produce a desired amount of lift, is maintained from entry interface to parachute deploy. Note that the EDLSA ellipsled produces maximum lift at a 55° total angle of attack.[5] Angles of attack greater than this were explored in the design space but were considered invalid.
2. The entry vehicle has sufficient control authority to maintain such an orientation and flight path angle.
3. A skip-out margin of 3° was specified to ensure skip-out would not occur. That is, a valid trajectory must have an entry flight path angle at least 3° greater than the flight path angle that results in skip-out.
4. Convective and radiative heat margins of 1.30 and 1.50, respectively, were applied.
5. Bank angle modulations are modeled as instantaneous step functions.

An initial design parameter space was established to explore a range of trajectories bounded by lift-up and lift-down orientations. Velocities at entry interface were fixed at 7.2 km/s. Selected entry flight path angles ranged between -7.0° and 0.0°, total angles of attack ranged between 0°

and 60°, and bank angles ranged between 0° and 180°, where 0° is lift-up and 180° is lift-down. Each trajectory was run in POST2 and analyzed in MATLAB. Though dependent on the magnitude of the lift vector, which is in part determined by the total angle of attack, lift-up trajectories are generally characterized by low g-loads, low heat rates, high total heat loads, and greater likelihood of atmosphere skip-out. Lift-down trajectories, conversely, are generally characterized by high g-loads, high heat rates, low total heat loads, and lower likelihood of atmosphere skip-out.

Figure 6 and Figure 7 show peak g-load and peak heat rate variations across bank angles and total angles of attack at a given entry flight path angle for the robotic and manned missions. It can be seen that as the entry flight path angle becomes steeper, the peak g-load at a given bank angle and total angle of attack increases. In fact, at an entry flight path angle of -7.0°, there is no combination of bank angle and total angle of attack that produces a peak g-load below 10 for either robotic or manned missions. Similarly, steeper flight path angles produce higher heat rates. In general, the "sweet spots" correspond to regions of shallow flight path angles with mid to high angles of attack and near-lift-up orientations.

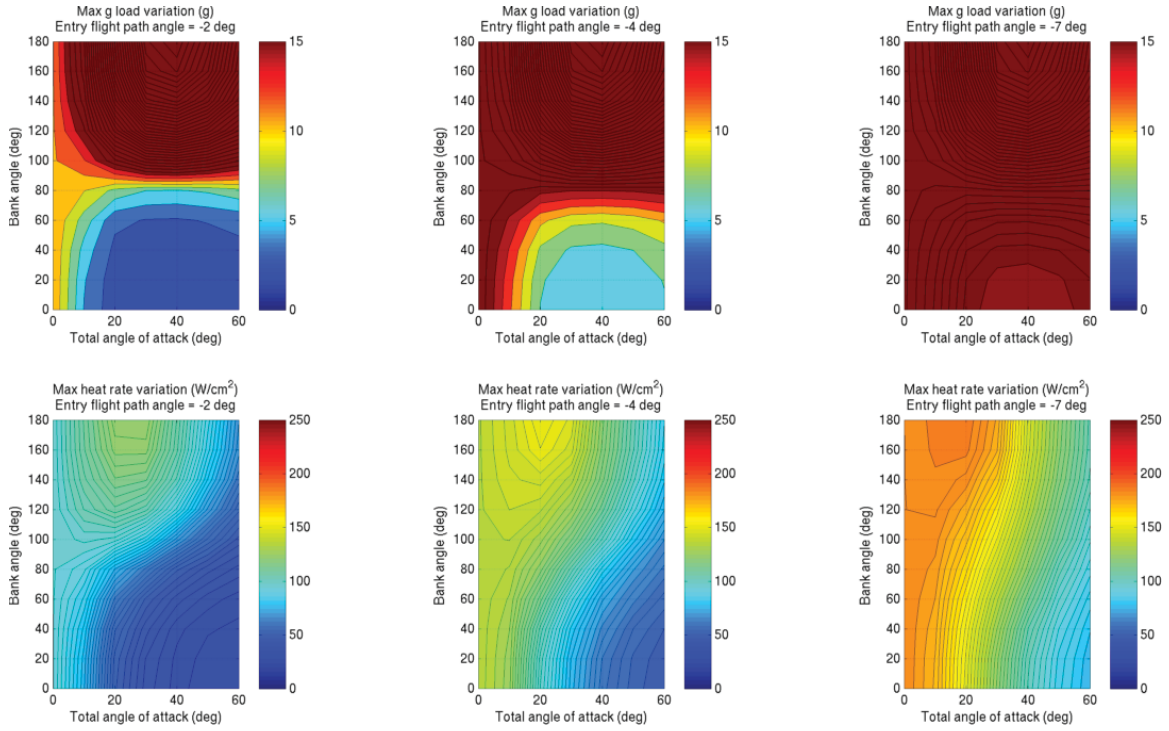

Figure 6. Robotic mission trajectory design space at selected flight path angles. Note that any values that exceed the range of the legend remain dark red or dark blue.

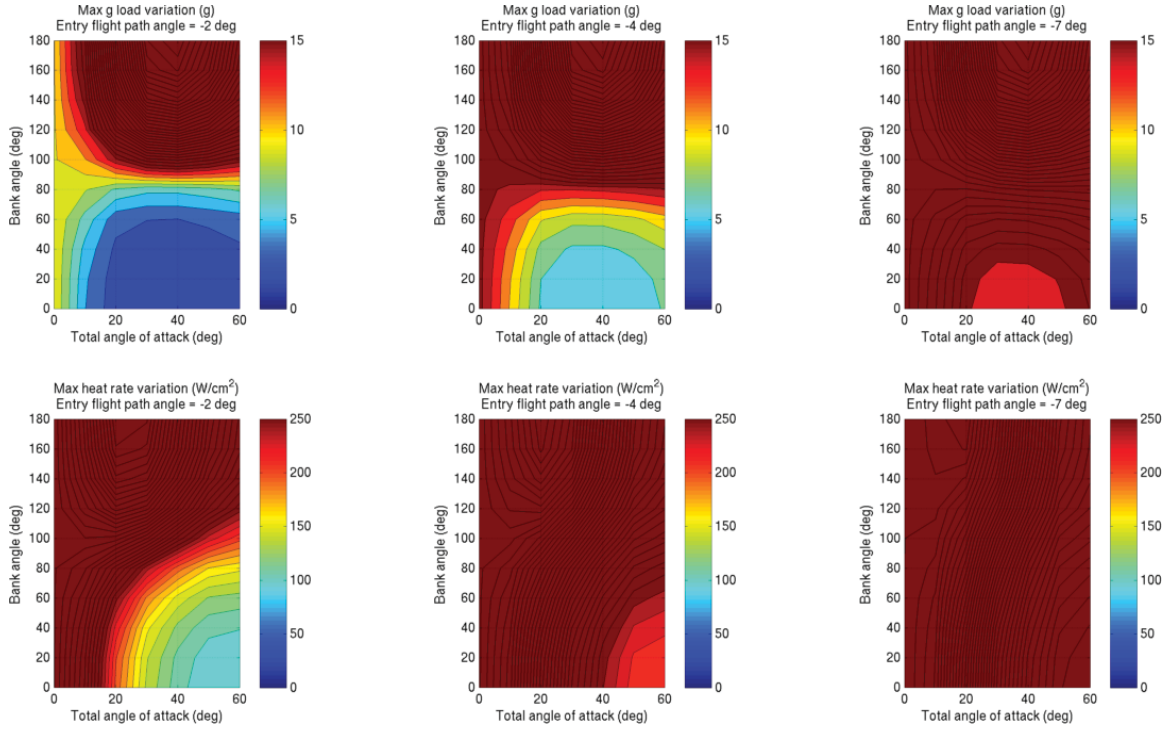

Figure 7. Manned mission trajectory design space at selected flight path angles. Note that any values that exceed the range of the legend remain dark red or dark blue.

Many of the valid trajectories obtained from the initial design space, exhibited two characteristics that necessitated adjustment of the entry profile: lofting and excessive g-loads. To counter the lofting behavior, a basic control logic algorithm was implemented in which the vehicle bank angle was modulated to near 90° if the altitude began to increase, which effectively rotates the lift vector away from near-vertical, or lift-up, thereby reducing the increase in altitude due to lift. Excessive g-loads were also mitigated by bank angle modulation, though in the opposite sense. That is, the bank angle was modulated to near 0° if the g-loads became excessive, which effectively rotates the lift vector towards the lift-up orientation. The result is a bank angle modulation profile that mitigates both lofting and excessive aerodynamic forces. To enable a clean deployment of the parachute, the final modulation is to a bank angle of 0° just prior to parachute deploy. Total angle of attack is also set to 0° to eliminate any lift.

A disc-gap-band (DGB) supersonic parachute, which was the assumed aerodynamic decelerator of choice for the HAVOC missions, may in general be deployed at Mach numbers between 2.25 and 1.00 and dynamic pressures between 900 and 200 Pa. The region in altitude-velocity space bounded by these limits is often referred to as the "Mach-q box" and is shown in Figure 8. Exceeding these conditions increases the probability that the parachute will either be destroyed due to excessive loading or exhibit areal oscillations that decrease efficiency of the parachute. Note the relatively low range of altitudes and velocities in the Mach-q box, the significance of which will be discussed later.

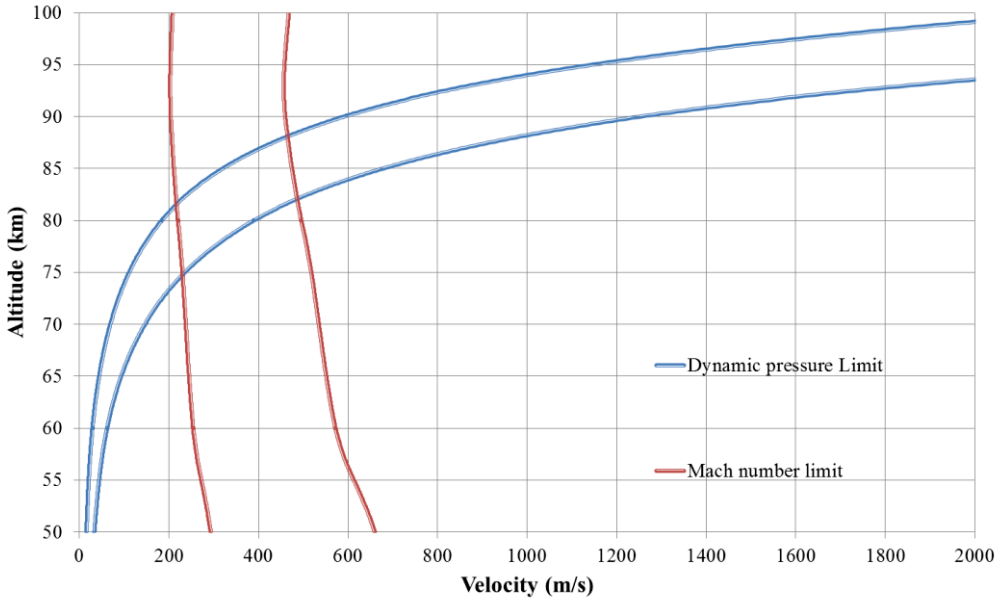

Figure 8. Venus Mach-q parachute box for (VenusGRAM 2005 atmosphere).

The purpose of the entry and descent portion of the trajectory is to place the EV at a condition that permits deployment of the supersonic parachute, after which the airship may begin inflation under terminal parachute descent. To this end, the valid trajectories were evaluated at Mach 2.1 to establish if parachute deployment conditions were met.

Airship Inflation and Terminal Descent

The terminal descent portion of the trajectory begins after parachute deploy. A HAVOC Terminal Descent Model (HAVOC-TDM) was developed for analyzing how aerodynamic, buoyancy, and inertial forces combine to fix the terminal velocity of the vehicle concept during unpowered descent. Existing trajectory models were utilized for modeling the initial descent from orbit to parachute deployment. However, to ensure a smooth transition between separate modeling tools, HAVOC-TDM does provide the option of moderate-fidelity modeling of the aerodynamic conditions prior to the time of parachute deployment. Table 2 lists relevant assumed parachute and airship parameters.

Table 2. Parachute and airship parameters.

Parameter	Unit	Unmanned	Manned
Supersonic Parachute			
Diameter	m	10	24
Supersonic drag coeff.	--	0.9	0.9
Transonic drag coeff.	--	0.85	0.85
Subsonic drag coeff.	--	1.15	1.15
Airship			
Mass	kg	1,382	95,776
Packed volume	m^3	20	1258
Inflated volume	m^3	250	77521
Inflation rate	m^3/s	1	400

HAVOC-TDM determines the aerodynamic and buoyancy forces acting on the transforming vehicle configuration as a function of time at altitude increments of 500 m. Table 3 is an example output from the model, including the altitude, time segment, and cumulative descent time. In addition, a detailed table of the factors required to calculate drag force components, and the buoyancy, weight, velocity, and acceleration is provided upon completion of each analysis.

Table 3. Sample inflation and terminal descent parameters.

	entry	deploy	descent	descent	descent	descent	End 1	End 2	End
	Entry Start	Parachute Deploy	Parachute Open	Shell Cut	Inflate Start	Parachute Cut	Inflation Δ Time	Velocity zero	DESCENT
altitude, km	69.5	69.0	68.0	64.0	64.0	54.5	52.0	52.0	52.0
dtime, s	58.55	2.05	5.48	30.46	35.94	151.89	190.7	257.0	257.0
timeline, s	58.55	60.60	66.08	96.54	96.54	248.43	287.2	353.5	353.5

Various mission, vehicle, and subsystem input parameters are used to dictate the sequence of operational events and to specify the conditions associated with the onset of each event. During each step, the descent conditions are assessed to determine which events have already occurred and if another operational event should be initiated. Distinct modeling and calculations are applied to each phase of the descent as a result of characteristically different vehicle configurations, weights, and buoyancy forces. Thus, the descent analysis model follows a pattern of 1.) identifying the descent phase, 2.) calculating conditions, 3.) assessing event onset, and 4.) calculating the time to descend 500m.

Once the vehicle inflation phase begins, it is assumed that all entry shields and capsules are jettisoned to reduce the total system weight, and that helium gas inflates the HAVOC concept at a specified and constant volume rate. The buoyancy force is calculated assuming an atmosphere molecular weight of 43.58 g/mole (approximately 97% CO_2 and 3% N_2) and a helium lifting gas weight of 4.0 g/mole. Due to the significant mass of the lifting gas tanks, the lifting gas was assumed to be equally contained in multiple tanks which would operate in succession and be jettisoned upon depletion. This design assumption was determined to significantly slow the rate of descent.

Changing drag forces on the vehicle as a result of inflation are calculated, including parasite and air-mass drag. The descent drag, parachute drag, buoyancy, and vehicle weight are used to determine the time required to descend 500m for the existing conditions. Updates to these factors continue until the buoyancy to parachute drag ratio exceeds 90%, at which time the parachute is released. The vehicle descent rate increases for a short time period after the parachute is released, but the atmosphere density increases to provide buoyancy increases that exceed those caused by the additional lifting gas volume released during that same period.

The descent time to the point of neutral buoyancy is determined at the point that the buoyancy force equals the vehicle weight. However, descent may continue as a result of the momentum of the vehicle, which may or may not be inflated at that altitude. In this case, as the vehicle reverses to ascend toward the higher altitude of equilibrated neutral buoyancy, the minimum altitude and the descent time to that altitude are output.

It is also possible that the inflation rate permits inflation at altitudes below the level of neutral buoyancy. In this case, as the vehicle reverses to ascend toward the higher altitude of equilibrated neutral buoyancy, the minimum altitude and the descent time to that altitude are output. It is also possible that the inflation rate permits inflation at altitudes somewhat above the level of neutral

buoyancy, in which case the inflated airship is assumed to safely descend to the neutral buoyancy altitude.

Thermal Protection System

The thermal protection system (TPS) was sized based on the nominal trajectory heating profiles with a 25% margin added to the final mass. For the robotic mission, given a 4.7 m diameter cylinder and half-sphere nose cap with a total length of 14.1 m, and assuming that the TPS covers all of the spherical nose cap and half of the cylindrical body, the total area covered by the TPS is 121.45 m^2. For the manned mission, given a 10.0 m diameter cylinder and half-sphere nose cap with a total length of 30.0 m, and assuming that the TPS covers all of the spherical nose cap and half of the cylindrical body, the total area covered by the TPS is 549.78 m^2.

Two TPS candidates were investigated for both missions. The first, Heatshield for Extreme Entry Environment Technology (HEEET), is a dual-layer material, with a high-density outer "recession" layer woven in to a lower density "insulation" layer and 3D woven carbon fibers infused with phenolic resin. The HEEET heatshield thickness was calculated to keep the TPS-structural interface temperature below 315°C. HEEET is currently at a low technology readiness level (TRL), but technology development effort is underway to prepare HEEET for mission infusion. It is expected that HEEET will be robust enough to handle a dual heat pulse with a cold soak between the pulses, which would be in the HAVOC mission profiles (aerocapture – cold soak – atmospheric entry).

The second TPS candidate was Phenolic Impregnated Carbon Ablator (PICA), which is a monolithic resin-infused fiberform insulation.[13] PICA requires a strain isolation pad (SIP) to isolate it from the support structure. A thickness margin of 10% was added for recession uncertainty. The PICA heatshield thickness was calculated to keep the TPS-structural interface temperature below 250°C. Note that it is currently unknown if PICA can withstand a dual heat pulse with a cold soak between the pulses.

For the TPS support structure, a 5.08 cm, 4.4 pcf aluminum honeycomb truss sandwiched between 0.1 cm graphite/BMI facesheets was assumed for the robotic mission. The manned mission used a more robust 7.62 cm, 6.0 pcf titanium honeycomb truss sandwiched between 0.2 cm graphite/BMI facesheets.

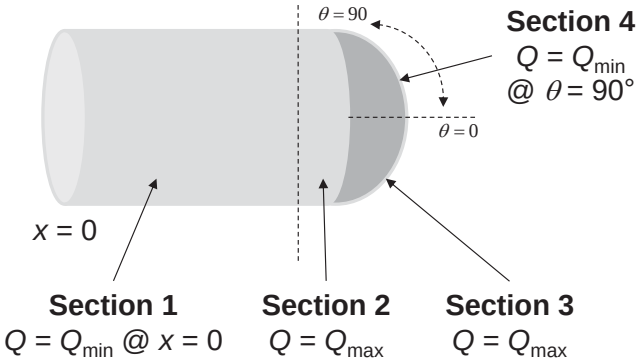

Figure 9. Moderate TPS tailoring.

Three different sizing techniques were used: constant TPS thickness, moderate thickness tailoring, and aggressive thickness tailoring. For the first, the TPS was sized to the peak heating location and the same thickness was used for the entire heat shield, resulting in a significant mass penalty. For the second, the TPS thickness was set piecewise given the expected heat profile

along the vehicle surface. Specifically, it was assumed that the heating fell off from maximum heating location to 60% of maximum value. Figure 9 shows how the TPS was divided into sections with different thicknesses. Sections 2 and 3 are of constant thickness and sections 1 and 4 are of variable thickness. Section 2 is 1.0 m long for the robotic case and 2.0 m long for the manned case.

The third TPS sizing technique was a more aggressive version of thickness tailoring. In this case, no TPS was used on the back side of the sphere or cylinder sections. The maximum TPS thickness was the intersection of the sphere and cylinder at the centerline. The thickness decreases from maximum to 60% of the heating value 2.35 m down the cylinder. Along the circumferential direction, the thickness decreases from maximum 60% of the heating value to the minimum thickness that can be manufactured, which is assumed to be 5.0 mm. Figure 10 shows how the heat shield is divided in this case.

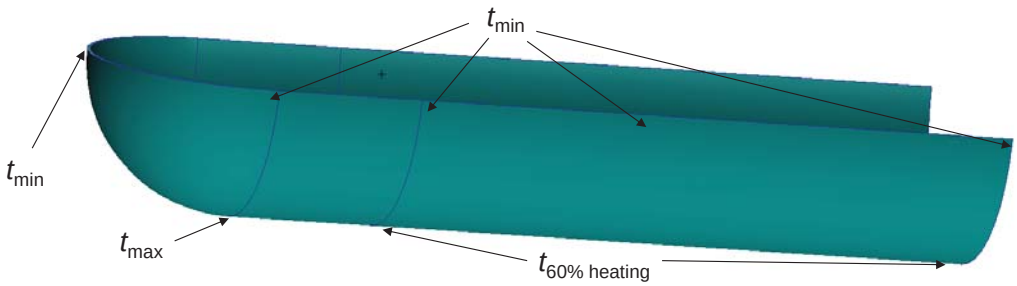

Figure 10. Aggressive TPS tailoring.

RESULTS

The overall trajectory design was an iterative process. First, the initial trajectory design space was generated and candidates were selected from the "pool" of initial conditions that satisfied the trajectory and mission requirements, e.g., presented low heat rates and g-loads. These candidates were deemed representative of nominal trajectories. These nominal trajectories, one for both the robotic and manned cases, were then used to size the TPS as previously discussed. The TPS sizing tool produces a new vehicle mass that is then used to re-run the trajectory design space, and the process is repeated until the TPS mass converges. Although further iterations would be required to fully close the design, the current results shown here represent HAVOC trajectories that deliver the desired payloads to the target altitudes.

Thermal Protection System

Table 4 lists the materials and values for the constant thickness approach for the robotic mission with a PICA heat shield at the end of the first iteration. Table 5 lists the materials and representative values for a HEEET heat shield for the same case. RTV-560 is a bonding agent.

Table 4. Representative properties of a PICA heat shield, robotic mission

Material	Thickness (cm)	Density (kg/m^3)	Mass (kg)	CBE+25% (kg)
PICA	4.9	273.9	1651.4	2640.3
RTV-560	0.03	1409.6	51.4	64.2
SIP	0.229	131.3	36.5	45.7
RTV-560	0.03	1409.6	51.4	64.2
Gr/BMI	0.1	1605.0	194.9	243.7
Al honeycomb	5.08	70.5	434.8	543.5
Gr/BMI	0.1	1605.0	194.9	243.7

Table 5. Representative properties of a HEEET heat shield, robotic mission

Material	Thickness (cm)	Density (kg/m^3)	Mass (kg)	CBE+25% (kg)
HEEET RL	0.2	1099.9	271.4	339.3
HEEET IL	2.79	824.4	2811.5	3514.4
RTV-560	0.03	1409.6	51.4	64.2
Gr/BMI	0.1	1605.0	194.9	243.7
Al honeycomb	5.08	70.5	434.8	543.5
Gr/BMI	0.1	1605.0	194.9	243.7

For the PICA TPS mass (with margin) is 2,238.3 kg and the structure is 1,030.9 kg, for a total of 3,269.2 kg. For the HEEET TPS mass (with margin) is 3,917.9 kg and the structure is 1,030.9 kg for a total of 4,948.8 kg. HEEET demonstrates a higher mass because it is more efficient at higher peak heat rates. Thus, for missions with relatively benign heating environments (such as the robotic HAVOC mission), in general PICA would be the preferred option due to its lower required mass.

A summary of the TPS sizing results using the three different techniques is listed in Table 6. Both PICA and HEEET are viable candidates for the robotic mission. PICA is the recommended option due to its lower mass. In the case of the manned mission, though PICA is lighter, it is approaching its heat flux limit. HEEET is also structurally stronger than PICA, and can tolerate much higher peak heat fluxes (on the order of 1,000 W/cm^2). Steepening the trajectory would increase the peak heat flux but reduce the total heat load and reduce the overall mass of the HEEET system in both the robotic and manned mission scenarios. Thus, despite having a higher mass, HEEET is the recommended option. The dual pulse capability must be experimentally verified for both materials.

Table 6. Summary of TPS masses.

	Robotic			Manned		
Material	Constant	Moderate	Aggressive	Constant	Moderate	Aggressive
PICA	2,238.3	2,124.6	1,329.4	14,151.2	13,536.1	11,813.2
HEEET	3,917.9	3,527.3	1,775.2	30,645.8	28,708.2	25,066.0

Using moderate TPS tailoring, the current EV mass (payload, airship, and aeroshell), is approximately 4,537 kg for the robotic mission (PICA) and 133.9 mt for the manned mission (HEEET). Using an aggressively tailored TPS permits a significant reduction in the overall TPS mass, providing the option to either have additional available payload mass or reduce the overall size of the vehicle.

Aerocapture Trajectory

Aerocapture inputs for the current mass iteration are listed in the Table 7. The lift-to-drag ratio was chosen to take full advantage of both the lift and drag area of the ellipsled vehicle, and the initial velocity and target were chosen based on the arrival opportunity from Earth and the desired initial EDI conditions.

Table 7. Nominal inputs for each system.

	Robotic	Human-Crewed	Human-Cargo
Lift-to-Drag Ratio	0.52	0.52	0.52
Initial Velocity	11.3 km/s	11.3 km/s	11.3 km/s
Target Orbit	300 km circular	300 km circular	300 km circular
Aeroshell Diameter	4.7 m	10 m	10 m
System Mass	4,537 kg	98 mt	128 mt

The nominal trajectories associated with each set of inputs produce g-loads and heat rates, shown in Figure 11, within the requirements of the system and the capability of the TPS material selected for this study. As the mass of the system increases from the robotic mission to the human-crewed mission, the peak heat rate value increases to reflect the change in ballistic coefficient. A heavier and larger diameter vehicle, entering the atmosphere at the same speed, requires more drag force in order to hit the same apoapsis target. To accumulate the necessary drag force, that vehicle must dive deeper into the higher density sections of the atmosphere, increasing the peak dynamic pressure and g-loads, and producing high peak heat rate values. Thus the peak heat rate values for the low mass robotic mission are much lower than those of the very high mass human missions.

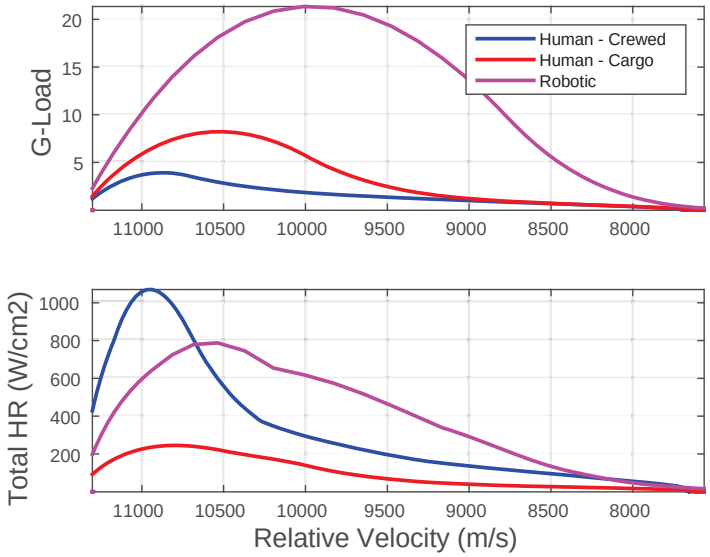

Figure 11. G-load and total heat rate values for each of the three systems.

Each of these trajectories delivers the vehicle into a 300 km circular orbit, enabling the EDI portion of the mission.

EDI Design Space

Table 8 lists relevant parameters from valid trajectories using moderately tailored thermal protection systems. The bolded lines are those deemed representative of a HAVOC trajectory and were selected as nominal. Entry conditions are the independent parameters that were varied in the design space. Bank modulation values, designed to mitigate lofting and excessive aerodynamic loads, were also varied. Peak loads and parachute deploy conditions are obtained from the simulated trajectories (recall that parachute deploy conditions are defined to be at Mach 2.1).

Table 8. Sample valid unmanned and manned trajectories.

Entry Conditions			Bank Modulation		Loads			Parachute Deploy Conditions (Mach 2.1)		
Bank angle	Angle of attack	Flight path angle	Bank (g)	Bank (alt)	Peak g-load	Peak heat rate	Total heat load	Altitude	Dynamic pressure	Relative velocity
deg	deg	deg	deg	deg	g	W/cm^2	J/cm^2	km	Pa	m/s
Robotic										
0	40	-4.25	0	70	6.105	119.24	9093	79.27	1494	466.04
0	40	-4.75	0	70	7.490	134.04	8582	79.29	1486	465.93
0	40	-4.75	20	70	7.731	135.27	8464	79.34	1470	465.69
0	50	-4.75	20	70	8.332	115.24	6639	82.46	713	452.35
10	50	-4.25	20	70	6.821	104.86	7093	82.03	791	453.91
10	**50**	**-4.75**	**20**	**70**	**8.366**	**115.46**	**6630**	**82.47**	**711**	**452.30**
20	50	-4.75	20	70	8.468	116.13	6606	82.51	704	452.16
20	50	-4.75	20	85	8.468	116.13	5782	79.17	1529	466.53
20	50	-3.50	20	70	4.845	87.51	7840	80.13	1230	461.99
Manned										
10	**50**	**-4.25**	**20**	**70**	**6.668**	**273.65**	**17760**	**74.07**	**4599**	**486.80**

Several trends in the parameters of interest may be identified from the table (only one manned mission is shown, though the same trends seen in the robotic mission results hold for this class of mission). Adjusting the entry angle of attack affects the final altitude: as angle of attack decreases, the final altitude decreases due to the EV having less lift (recall that peak lift is at a 55° total angle of attack). Thus, higher angles of attack are desirable to terminate at a higher altitude, where there is lower density and therefore lower dynamic pressure.

Adjusting the entry flight path angle has a small effect on final altitude, but a strong effect on g-load: as the entry flight path angle approaches zero, the g-load decreases, as expected. Thus, shallower entry flight path angles are desirable from a g-load mitigation standpoint, but steeper angles are desirable to avoid atmospheric skip-out. The entry flight path angle of -4.75 (robotic) and -4.25 (manned) listed in the table was selected because it was deemed a safe margin from skip-out while also providing survivable g-loads.

Other trends may be identified from the table. Increasing the entry bank angle increases the peak g-load but has a negligible effect on peak heat rate and final altitude. Increasing the target bank angle for loft mitigation has a negligible effect on peak heat g-load and peak heat rate, but decreases the final altitude, resulting in higher density and dynamic pressure. Increasing the target bank angle for g-load mitigation has negligible effect on peak heat rate and final altitude, but increases the peak g-load.

Thus, it is desirable to have an entry bank angle close to vertical, a high entry angle of attack, a shallow flight path angle, a bank angle modulation for g-load mitigation close to vertical, and a bank angle modulation for loft mitigation close to horizontal. This is supported by the design space results shown in Figure 6 and Figure 7.

Finally, it can be seen that none of the manned missions have a dynamic pressure at the Mach 2.1 condition that is between 200 and 900 Pa, which is required for supersonic parachute deploy. As will be discussed later, this issue must be addressed with the use of an additional aerodynamic decelerator. Nevertheless, it was of interest to examine these trajectories in further detail. Analysis of the terminal descent and airship inflation phase of the manned mission trajectory continued

under the assumption that an additional decelerator is used to establish feasible parachute deploy conditions.

EDI Trajectory

Trajectory results for the nominal HAVOC missions are shown in Figure 12 through Figure 14. Recall that these are not intended to be the proposed trajectory profiles, but rather show trajectories drawn from the many valid cases that fulfill the mission requirements. Figure 12 shows trajectory parameters for both classes of HAVOC missions. Lofting behavior is drastically mitigated from initial trajectories (though not completely eliminated) and brief altitude increases are restricted to below 100 km.

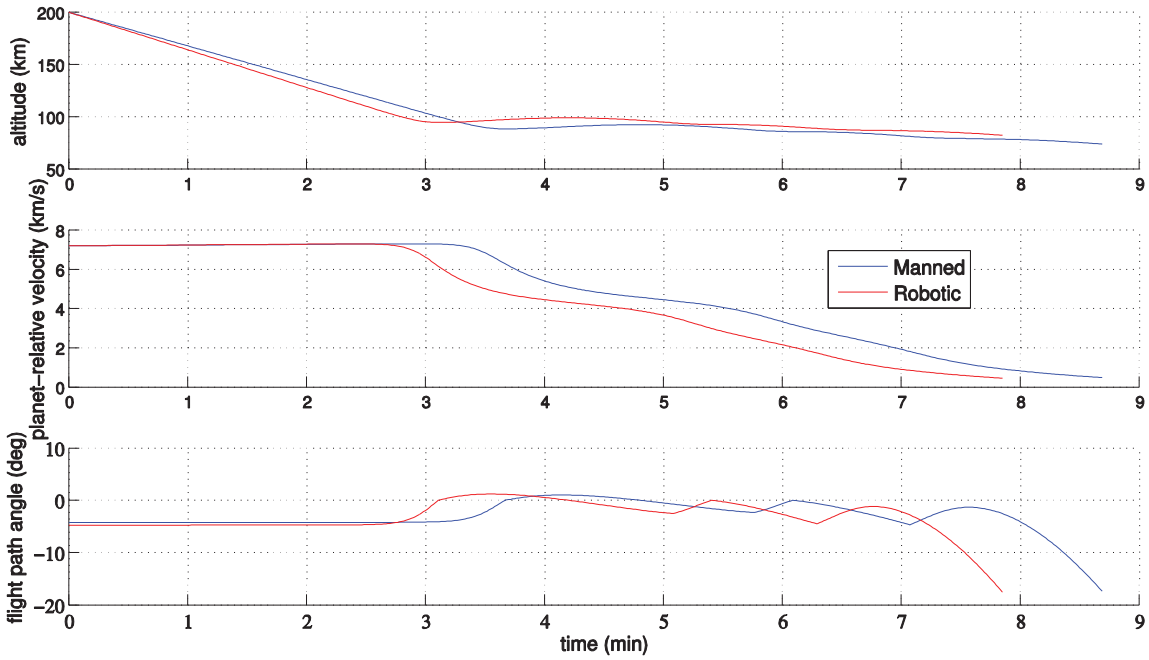

Figure 12. Trajectory parameters.

Figure 13 shows aerodynamic parameters for both classes of HAVOC missions. The most notable differences between the missions in these results are those between dynamic pressure and ballistic coefficient. The cause for the higher dynamic pressure for the manned mission is twofold. Figure 12 showed that a given time, the manned mission is both at a lower altitude and moving at a higher velocity due to the higher ballistic coefficient. Recalling that $q_\infty = \frac{1}{2}\rho_\infty V_\infty^2$, dynamic pressure is sensitive to changes in velocity. Combined with the higher density at lower altitudes, the dynamic pressure profile for the manned mission is significantly higher than that of the robotic mission. In fact, from Table 8, by the time the entry vehicle reaches the nominal chute deploy condition of Mach 2.1, the dynamic pressure is approximately 4.6 kPa. As will be discussed later, this dynamic pressure is too high for parachutes commonly used in EDL operations.

The two smaller peaks in dynamic pressure at approximately 6 and 7 minutes into the manned trajectory are caused by the slight lofting behavior seen in the top panel of Figure 12.

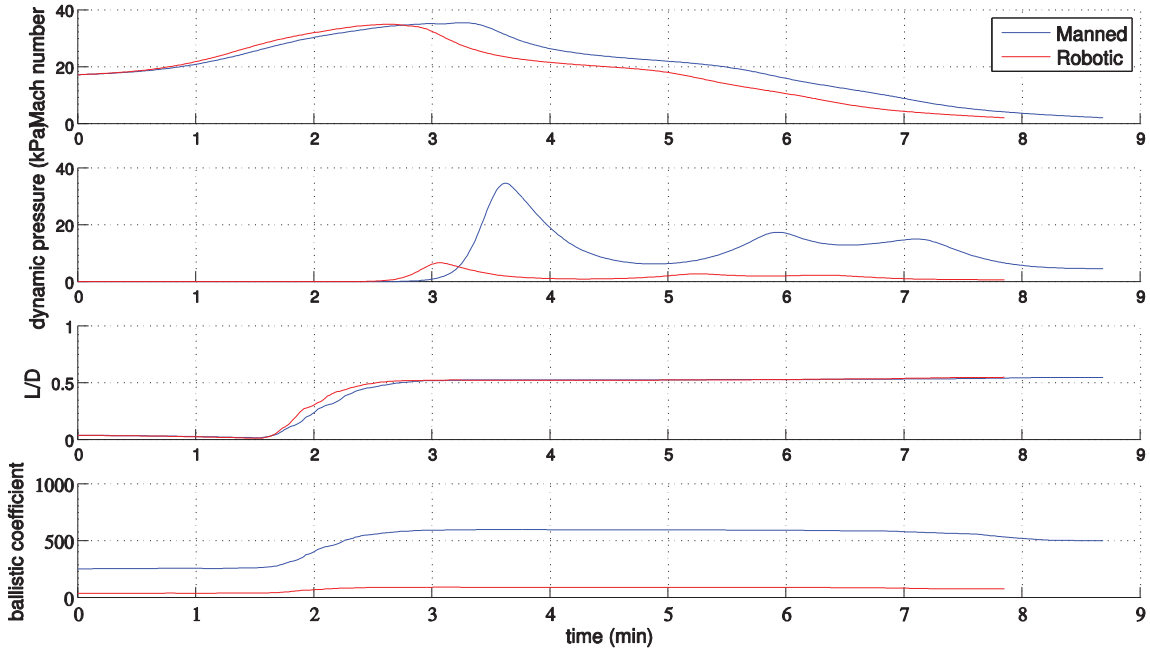

Figure 13. Aerodynamic parameters.

Figure 14 shows aerodynamic and aeroheating loads for both classes of HAVOC missions. The higher heat rates and correspondingly higher heat loads for the manned mission are evident. G-loads, shown in the bottom panel, illustrate the effects of the bank angle modulations designed to mitigate these loads.

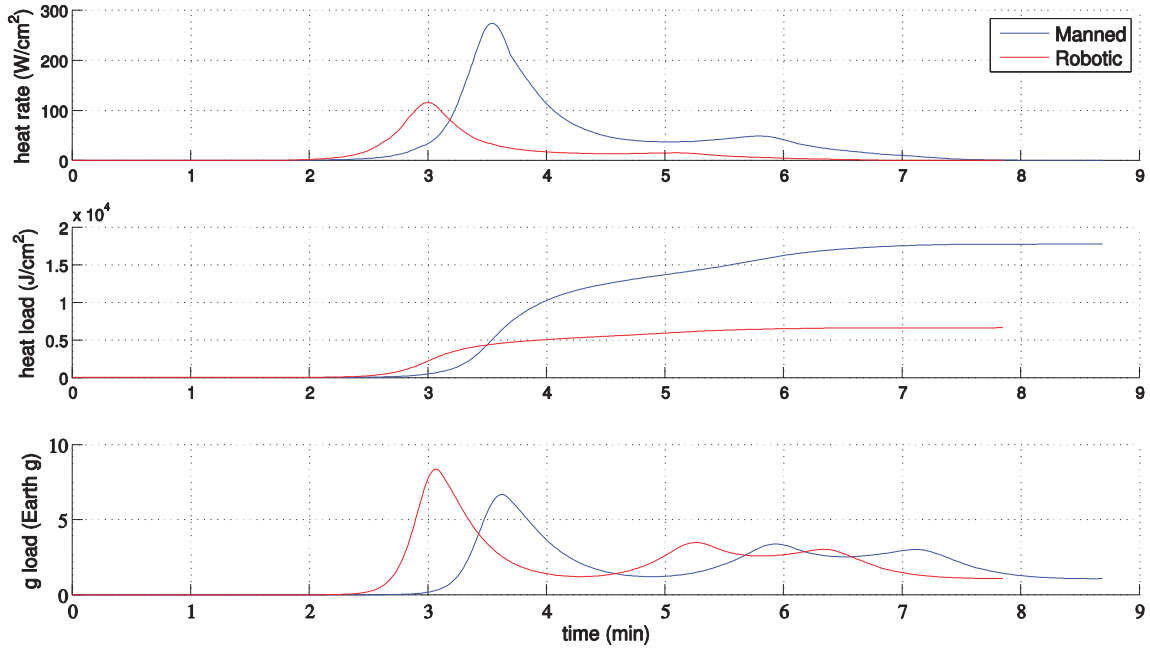

Figure 14. Aerodynamic and aeroheating loads.

Recall that the dynamic pressure at Mach 2.1 for the case of the manned missions well exceeded the 900 Pa limit of conventional supersonic parachutes. Despite this limitation, analysis of the terminal descent and airship inflation phase of the manned mission trajectory continued under the assumption that an additional decelerator may be used to establish feasible parachute deploy conditions.

Airship-related parameters during terminal descent and airship inflation is shown in Figure 15. These are shown as a function of altitude rather than time. Note the logarithmic scales on volume and drag force.

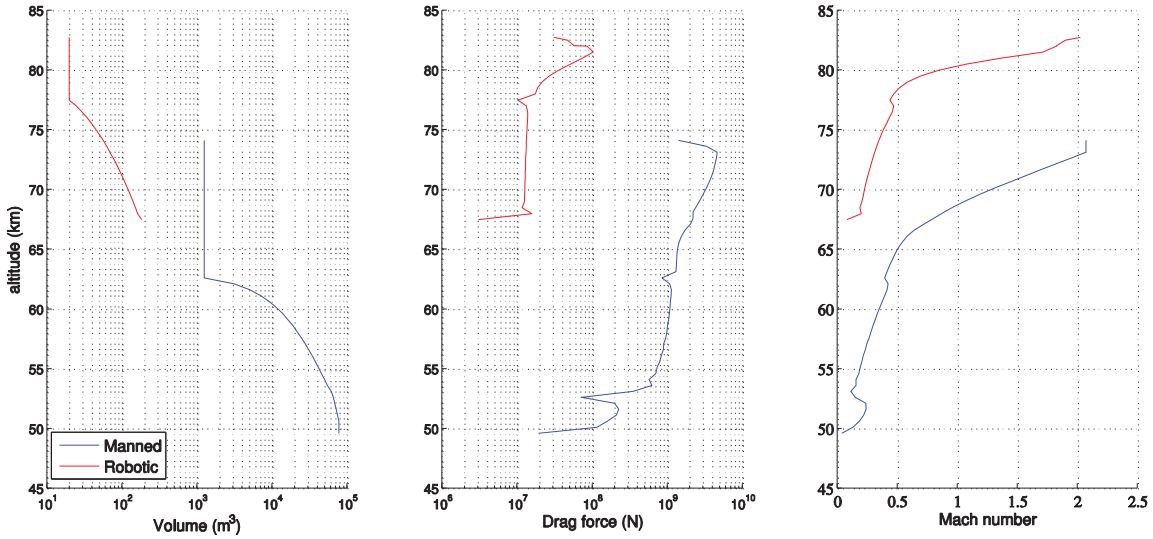

Figure 15. Terminal descent and airship inflation parameters.

The plots show several features of interest. Airship inflation begins when the descent speed becomes less than 100 m/s and then continues at a constant rate (listed in Table 2) until the airship is fully inflated. Full inflation occurs at an altitude different than the targeted 50 km. The neutral buoyancy condition of the airship, however, is designed to be 50 km, and so in both cases the airship will continue to descend or ascend until it settles at the target altitude.

The drag force profiles exhibit two sudden decreases at 77.4 km and 67.5 km for the robotic case and at 62.6 km and 52.6 km for the manned case. These correspond to aeroshell and parachute jettison, respectively. In the case of the robotic mission, the parachute is jettisoned just prior to full inflation (recall that the parachute is jettisoned when the buoyancy force reaches 90% of the parachute drag). Corresponding increases to the Mach number at these altitudes are also apparent.

SUMMARY AND CONCLUSIONS

A trajectory design and analysis that describes aerocapture, entry, descent, and inflation of manned and unmanned Venus lighter-than-air missions has been presented. Analysis of point cases drawn from the manned mission design space showed that dynamic pressures at parachute deploy exceed the valid environment due to the relatively low altitude at which the vehicle reaches Mach 2.1, and resultant high density. The high dynamic pressure is beyond the survival capability of commonly used parachutes (such as disc-gap-band) used in current planetary exploration. Thus, a different technology such a ribbon parachute or ballute must be used to slow the vehicle enough to permit the airship to inflate while under a parachute. In the case of the unmanned,

robotic lighter-than-air mission to Venus, it was determined that such a mission is feasible using current and near-future technology, such as a PICA thermal protection system. Future work will include implementation of guidance and control systems aboard the entry vehicle to aid in refining the reference trajectories. For the manned mission this may improve the dynamic pressure at the Mach 2.1 condition and enable the use of a conventional supersonic parachute.

ACKNOWLEDGEMENTS

The authors thank Dr. Juan Cruz of NASA Langley Research Center for discussions and suggestions on parachute technologies, and Dave Helton, Bob Evangelista, Chris Keblitis, Kevin Greer, Josh Sams, and Leanne Troutman of the Advanced Concepts Lab at NASA LaRC for vehicle renderings and imagery.

REFERENCES

[1] Committee on the Planetary Science Decadal Survey, Space Studies Board, Division on Engineering and Physical Sciences, *Vision and Voyages for Planetary Science in the Decade 2013-2022*, The National Academies Press, Washington, D.C., 2011.

[2] Limaye, S., *et al*., "Venus White Paper for Planetary Sciences Decadal Survey Inner-Planets Panel: Venus Exploration Goals, Objectives, Investigations, and Priorities," VEXAG (Venus Exploration Analysis Group) Executive Committee, 2009.

[3] Brauer, G. L., Cornick, D. E., and Stevenson, R., "Capabilities and Applications of the Program to Optimize Simulated Trajectories (POST)," NASA CR-2770, 1977.

[4] Striepe, S. A., *et al.*, *Program to Optimize Simulated Trajectories (POST2)*, Vol. 2: Utilization Manual, Ver 3.0.NESC, NASA Langley Research Center, Hampton, VA, May 2014.

[5] Dwyer Cianciolo, A. M., *et al*., "Entry, Descent and Landing Systems Analysis Study: Phase 1 Report," NASA Technical Memorandum, July 2010, NASA/TM-2010-216720.

[6] Justh, H. L., Justus, C. G., and Keller, V. W., "Global Reference Atmospheric Models, Including Thermospheres, for Mars, Venus, and Earth," AIAA/AAS Astrodynamics Specialist Conference and Exhibit, Keystone, CO, August 2006, AIAA 2006-6394.

[7] NASA Space Flight Human-System Standard, Volume 2: Human Factors, Habitability, and Environmental Health. NASA, 2011, NASA-STD-2001.

[8] Drake, B. G. (ed.), "Human Exploration of Mars Design Reference Architecture 5.0," Mars Architecture Group, NASA Headquarters, July 2009.

[9] Kinney, D. J., "CBAERO 4.1+ User's Manual," Systems Analysis Branch, NASA Ames Research Center, CA, September 2012.

[10] Kinney, D. J., Garcia, J. A., and Huynh, L., "Predicted Convective and Radiative Aerothermodynamic Environments for Various Reentry Vehicles Using CBAERO", 44th AIAA Aerospace Sciences Meeting and Exhibit, Reno, Nevada, 2006.

[11] Mazaheri, A., Gnoffo, P. A., Johnston, C. O., and Kleb, B., "LAURA Users Manual: 5.5-65135," Langley Research Center, Hampton, Virginia, February 2013.

[12] Nichols, R. H. and Buning, P. G., "User's Manual for OVERFLOW 2.2," August 2010.

[13] Tran, H. K., *et al*., "Phenolic Impregnated Carbon Ablators (PICA) as Thermal Protection Systems for Discovery Missions," NASA Technical Memorandum, April 1997, NASA/TM-110440.